„Meteor" Forsch.-Ergebnisse	Reihe A	No. 18	Seite 13—22	Berlin · Stuttgart	November 1976

Estimation of current and temperature coherence in the Norwegian Sea

by

Henry Perkins, School of Marine and Atmospheric Sciences, University of Miami, and
Gerold Siedler, Institut für Meereskunde, Kiel

With 9 figures and 2 tables

Bestimmung der Kohärenz von Strömung und Temperatur in der Norwegischen See

Zusammenfassung

Strömungs- und Temperaturdaten der Expedition „Norwegische See 1969" werden in bezug auf die Kohärenz für unterschiedliche Vertikal- und Horizontalabstände untersucht. Die vertikale Kohärenz zeigt den bekannten Zusammenhang abnehmender Kohärenzgrenzfrequenz mit zunehmendem Instrumentenabstand. In diesem Gebiet mit starken Scherströmungen und Bodenneigungen findet man jedoch eine kleinere vertikale Kohärenz als bei Daten, die unter Verhältnissen erhalten wurden, die typisch für den offenen Ozean sind. Bei einer Darstellung der zirkular polarisierten Strömungskomponenten findet man keine verstärkte Kohärenz für im Uhrzeigersinn rotierende Komponenten, obwohl sie energiereicher als die gegen den Uhrzeigersinn drehenden Komponenten sind. Das Verhältnis der spektralen Energie für die im und gegen den Uhrzeigersinn rotierenden Komponenten entspricht demjenigen, das für lineare interne Wellen zu erwarten ist. Die Kohärenz ist für die halbtägige Gezeit im allgemeinen signifikant von Null verschieden und die Phase nahe Null. Das paßt zu überwiegend barotropen Bewegungen. Es wird gezeigt, daß barokline Gezeitenbewegungen zu gewissen Zeiten als Folge der Änderung des zulässigen Frequenzbereichs für freie interne Wellen durch die lokale mittlere Stromscherung nicht existieren dürften.

Summary

Current and temperature data gathered during the expedition "Norwegian Sea 1969" are described in terms of coherence over various vertical and horizontal separations. Vertical coherence estimates display the well-known trend of decreasing cut-off frequency with increasing instrument separation but are lower in this region with strong shear flow and sloping bottom than those that have been observed under typical open ocean conditions. In terms of circularly polarized current components, there is no enhanced coherence for currents rotating clockwise, although they are more energetic than those rotating anti-clockwise. The ratio of clockwise to anti-clockwise spectral energy is consistent with that expected from linear internal wave dynamics. Coherence for the semi-diurnal tide is usually significant, and the phase is close to zero, suggesting mainly barotropic motion. It is shown that baroclinic semi-diurnal tidal motion should be excluded at certain times due to the modification by local mean shears of the frequency range in which free internal waves are allowed.

1 Introduction

Cross-spectral properties of current variations at different positions in the ocean are a measure of spatial scales of inherent processes. It is usually assumed that the range between inertial and Väisälä frequency is mainly governed by internal wave dynamics and less by turbulence. This was first documented by Fofonoff (1968) and subsequently incorporated in a universal spectral shape by Garrett & Munk (1972, 1975) who attempt to describe the three-dimensional field of motion in this frequency range from observed auto- and cross-spectral data on the basis of random phase internal waves.

Major tools for studying spatial variations in the current field are moored arrays. Results on horizontal and vertical coherences from such arrays were recently summarized by Siedler (1974), indicating

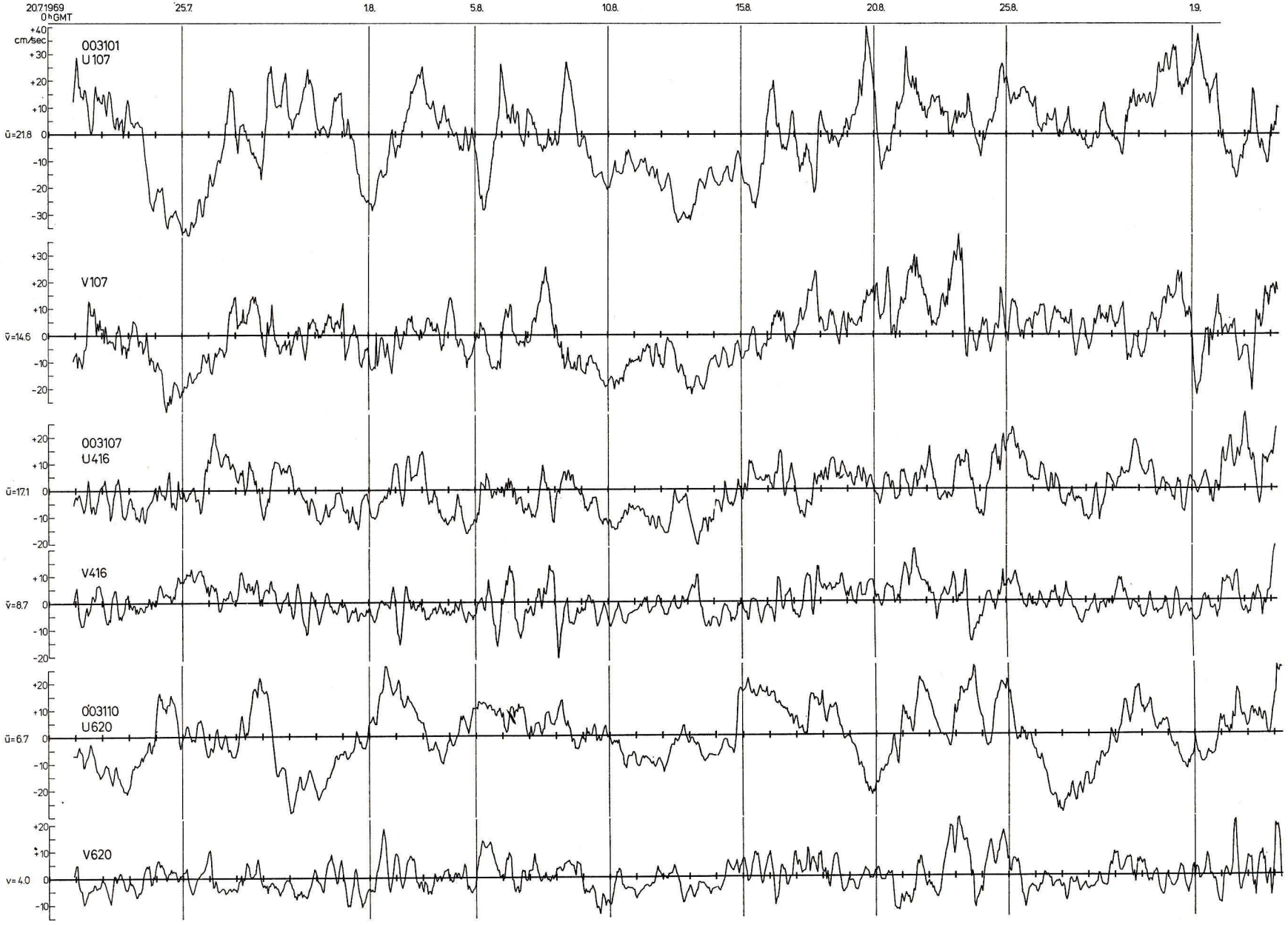

Fig. 2. Time series of currents at the depth levels 107, 416, and 620 m on mooring III. Mean for total record length subtracted and indicated on the left side.

Abb. 2. Zeitserien der Strömungen in den Tiefen 107, 416 und 620 m bei Verankerung III. U = Ost-West-Komponente. V = Nord-Süd-Komponente. Mittelwerte für die gesamte Registrierdauer sind abgezogen und auf der linken Seite angegeben.

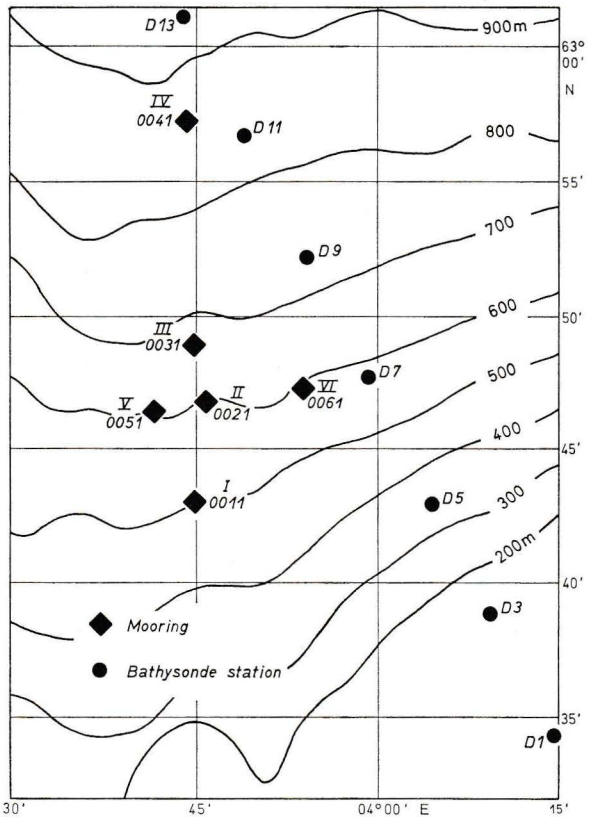

Fig. 1. Bathymetric chart of the observation area with location of moorings I—VI.

Abb. 1. Tiefenkarte des Beobachtungsgebiets mit den Positionen der Verankerungen I—VI.

that a loss of correlation for increasing separations is typical for open ocean conditions. The data from the Norwegian Sea Expedition 1969 (DIETRICH & HORN 1973) used for the present study provide the possibility of determining such properties in a region with strong mean current speed and strong shear over a sloping bottom. During this experiment six current/temperature meter moorings were set on lines approximately normal and parallel to the isobaths on the continental slope off Norway (fig. 1). The depths varied from 505 to 872 m. The separations of mooring positions were approximately 2, 4 and 8 nautical miles, and the approximate levels of meters were 110, 160, 210, 310, 360, 420, 470, 570, 620 and 770 m. Usable record length was typically 44 days although some records were shorter due to technical problems. More details of the array and of hydrographic soundings made during the cruise are given by DIETRICH & HORN (1973).

2 The data

As a compilation of the complete set of current and temperature data has been prepared by HORN & SCHOTT (1975), only a few typical examples of the data will be given here to facilitate the later discussion of cross-spectral properties. Data from mooring no. III ($\varphi = 62° 48{,}9'$ N, $\lambda = 3° 45{,}1'$ E) for three depth levels were selected for this purpose.

The time series of currents (fig. 2) display certain features of the temporal variability: Fluctuations on scales of a few days with particularly large amplitudes in the east-west components, semi-diurnal tidal changes and fluctuations in a broad range of shorter scales. This corresponds to usual current variations in the deep ocean. A sample spectrum, typical of those obtained throughout the array, is given in fig. 3 (for an explanation of rotating coordinates see chapter 3).

Table 1 42 day-average vertical shear from 100 to 500 m at each site for downstream component of current. Positive values indicate current increasing with depth.

Mooring	Shear ($sec^{-1} \times 10^{-5}$)	Mooring	Shear ($sec^{-1} \times 10^{-5}$)
I	+5	IV	−36
II	−25	V	−30
III	−27	VI	−10

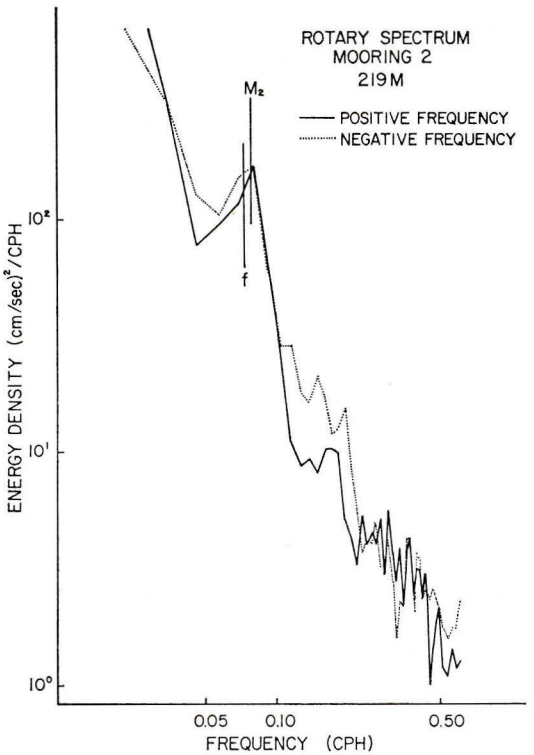

Fig. 3. Rotary spectrum for positive and negative frequencies corresponding to circularly polarized current components rotating in the anti-clockwise and clockwise directions, respectively.

Abb. 3. Spektrum der rotierenden Komponenten für positive und negative Frequenzen entsprechend zirkular polarisierten Strömungskomponenten mit einer Rotation entgegen bzw. mit dem Uhrzeigersinn.

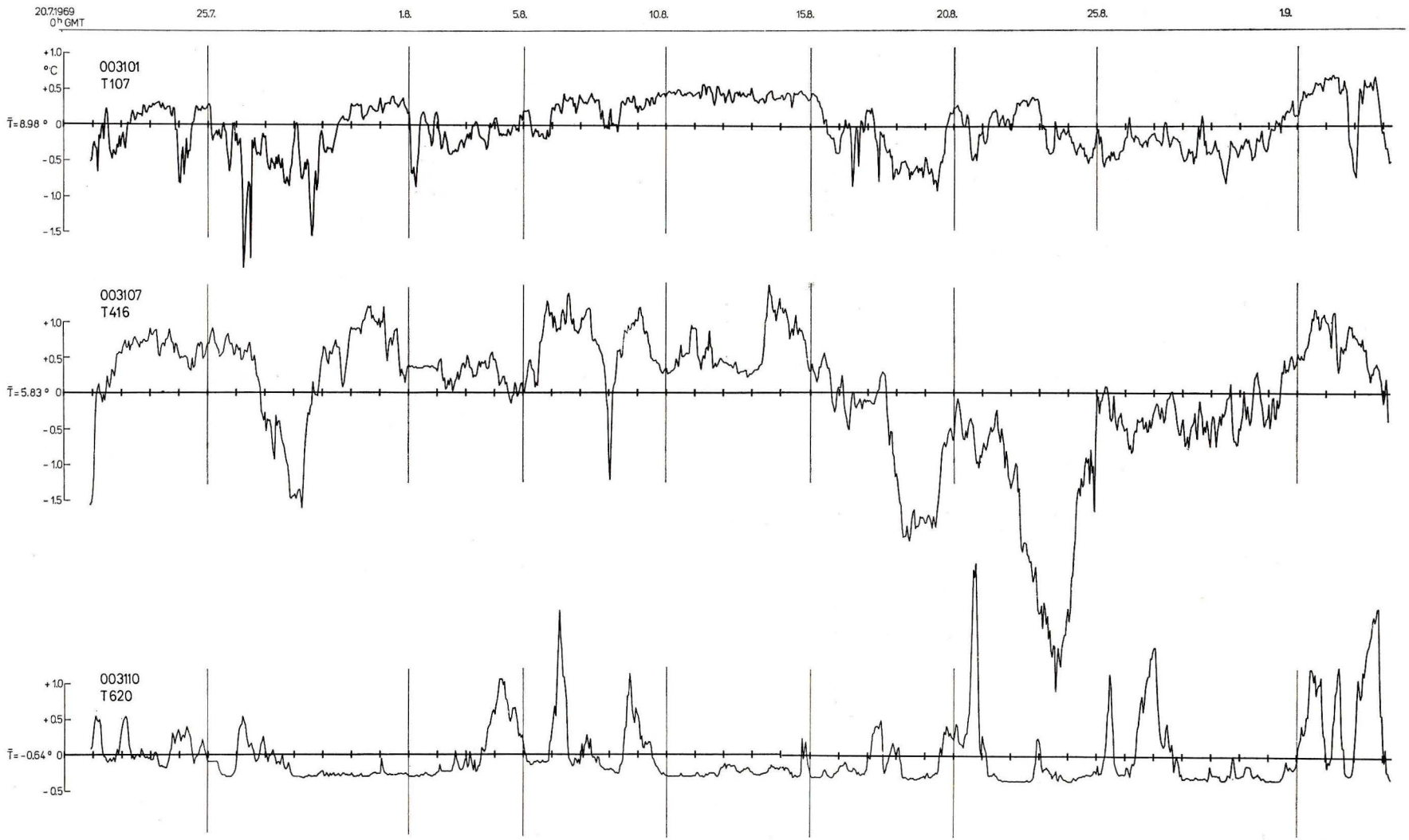

Fig. 5. Time series of temperatures T at the depth levels 107, 416, and 620 m on mooring III. Mean values for the total record length are subtracted and indicated on the left side.

Abb. 5. Zeitserien der Temperaturen T in den Tiefen 107, 416 und 620 m bei Verankerung III. Mittelwerte für die gesamte Registrierdauer sind abgezogen und auf der linken Seite angegeben.

Table 2 42 day-average horizontal current shear in downstream component of current at various depths between selected pairs of stations. Units are $sec^{-1} \times 10^{-5}$. In all cases, currents are stronger at the first-numbered mooring than at the second.

Moorings	Depths (approx.)		
	150 m	300 m	500 m
I, II	0,4	0,8	1,9
I, V	—	1,4	2,5
II, III	0,8	1,7	0,5
III, IV	0,5	0,8	0,8

The mean currents, however, have specific properties here as shown by the progressive vector diagrams in fig. 4. The Norwegian Current appears to be extremely steady during the period of observation, and strong current shear is found in this area. Tables 1 and 2 summarize 42 day-average shears in the vertical and cross-stream directions respectively as calculated from the profiles given by HORN & SCHOTT (1975). The tendency is clear for currents to be strongest towards the bottom at the shallowest mooring (no. I) and towards the surface at the deepest mooring (no. IV), with a systematic reversal in be-

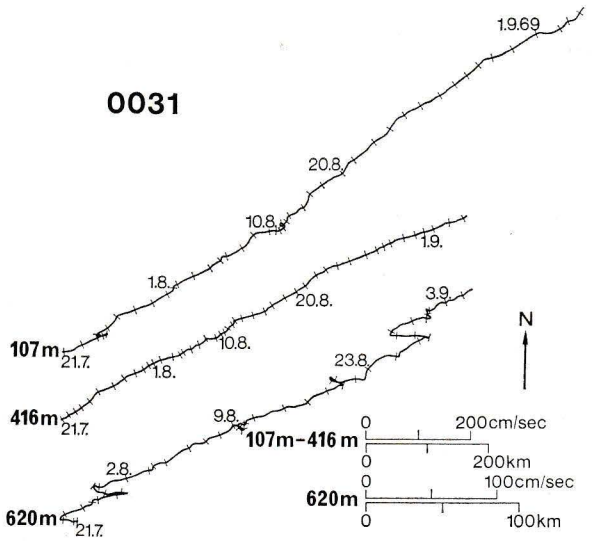

Fig. 4. Progressive vector diagrams of current at the depth levels 107, 416, and 620 m on mooring III, based on hourly means. Bars indicate 1-day intervals, and speed scales indicate mean speeds between bars.

Abb. 4. Progressive Vektordiagramme der Strömungen in den Tiefen 107, 416 und 620 m bei Verankerung III, berechnet mit einstündigen Mittelwerten. Die Strichmarken zeigen 1-Tag-Intervalle an, die Geschwindigkeitsskalen beziehen sich auf mittlere Geschwindigkeiten zwischen den Strichmarken.

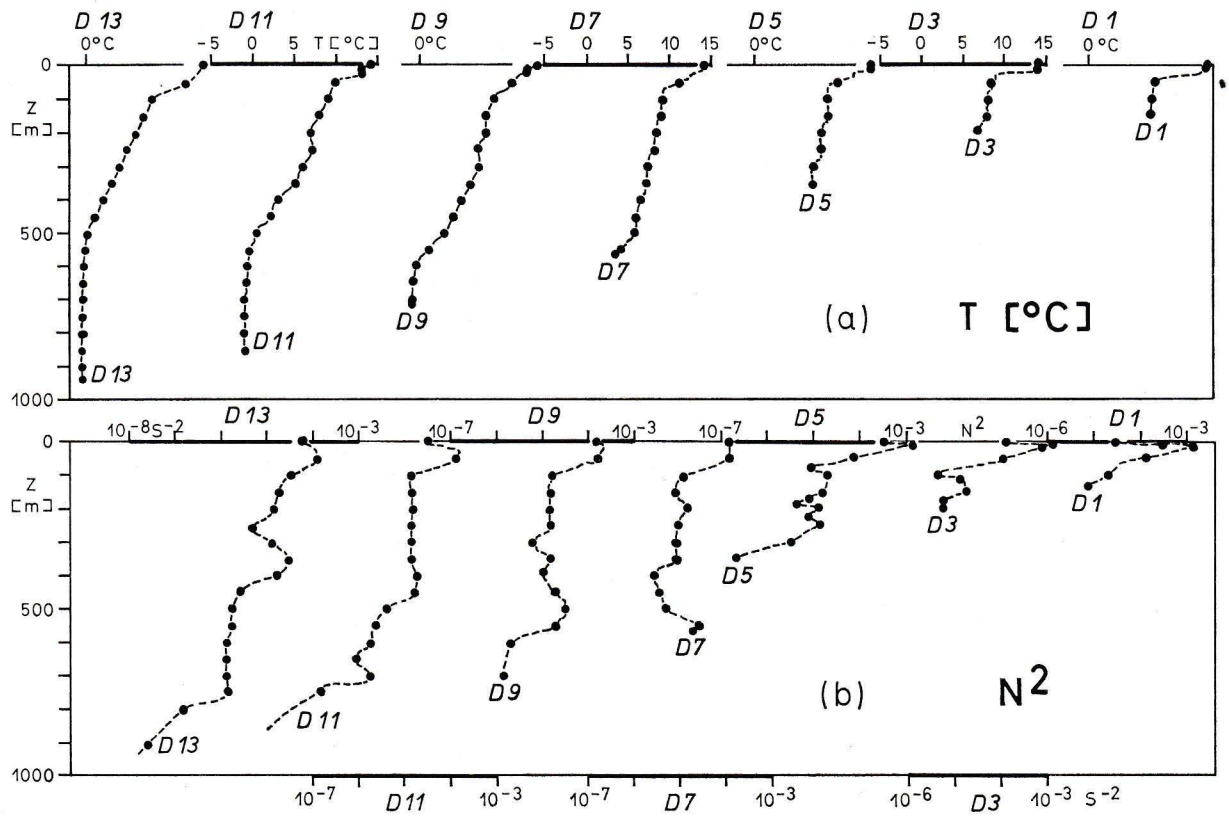

Fig. 6. Vertical mean profiles of temperature T and Väisälä frequency squared N^2. Each profile shown results from averaging over 6 profiles repeated during a period of 5 days.

Abb. 6. Mittlere Vertikalprofile der Temperatur T und der quadrierten Väisälä-Frequenz N^2. Jedes gezeigte Profil wurde durch Mittelung über 6 Profile, die während eines Zeitraums von 5 Tagen wiederholt wurden, gewonnen.

tween. Horizontal shears are estimated at the three depth horizons by taking the difference of the average velocity of selected pairs of instruments divided by their component of separation in a direction transverse to that of the mean current. Note that without exception the horizontal shears become stronger with increasing depth while they tend to weaken in the offshore direction at the two deeper levels. In all cases, the sense of the shear implies an increase of current with decreasing water depth.

Temperature time series corresponding to the current time series of fig. 2 are given in fig. 5. Mean temperature profiles for a section normal to the continental slope are given in fig. 6a for comparison. There are two depth ranges with large vertical temperature gradients. The meter at 107 m was placed in the lower portion of the upper high gradient range, the seasonal thermocline. The meter at 416 m detected particularly large temperature variations because of its position in the upper portion of the lower high gradient range where also high horizontal temperature gradients are found. The meter at 620 m was usually, but not always, below this lower high gradient range which explains the asymetric trace of this record. Apart from these differences due to the properties of the mean temperature profile, the records are similar to the current records in fig. 2.

The average Väisälä frequency distribution resulting from profiles of temperature and salinity is given in fig. 6b. Salinity plays a role close to the shelf edge while the Väisälä frequency is mainly controlled by the temperature distribution further off the slope.

3 Procedure for estimating cross-spectra

Computations of cross-spectra for pairs of vector time series requires some extension of the customary techniques used for pairs of scalar series. Straightforward application of scalar series techniques to the four possible pairs of Cartesian components is not generally satisfactory since the results depend on the choice of coordinate system in which the two series were decomposed. We use instead a version of the method described by MOOERS (1973) and by GONELLA (1972), briefly summarized as follows:

Let the complex current, $U = u + i\,v$, where u and v are respectively the east and north components of current, be represented by P nonoverlapping portions of N points each, thus forming a series of complex numbers, $U_{p,j}$; $p = 1, \ldots P$; $j = 0, \ldots N-1$, which represents the current at a fixed location. The division of the series into nonoverlapping pieces is done so that each piece may be treated as an independent representation of the basic series for statistical purposes. More generally, pairs of such series must be considered and are denoted by

$$U^{(l)}_{p,j}\ l = 1,2$$

where l implicitly associates the series with some point in space, $\underset{\sim}{x}_l$. Each piece of both series may then be represented by a complex Fourier series

$$U^{(l)}_{p,j} = \sum_{K=-N/2}^{+N/2} A^{(l)}_{p,K}\ \exp(i\,\omega_K\,t_j)$$

where $\omega_K = -\dfrac{2\,\pi\,K}{N\Delta t}$ and N is assumed to be even.

For interpretive purposes, note that $\exp(i\,\omega_K\,t_j)$ sweeps out a circle in the complex plane as j takes on successive values; clockwise for ω_K negative, counterclockwise for ω_K positive. Hence, the complex Fourier coefficients, $A^{(l)}_{p,K}$, have magnitude equal to the radius of the corresponding current circle and phase corresponding to the current direction at time $t = 0$.

The ensemble average of a quantity, x, is estimated by the arithmetic mean over all available pieces; that is, by

$$\langle\alpha\rangle = \langle\alpha_p\rangle = P^{-1}\sum_{=1}^{P}\alpha_p$$

The two-sided, complex cross-spectrum between series i and j may then be defined as

$$s^{(i,j)}_K = \langle A^{(i)}_{p,K}\,A^{(j)*}_{p,K}\rangle$$

where * denotes complex conjugation. Each term in this average thus has magnitude equal to the product of the magnitudes of the two complex Fourier coefficients and has phase equal to the difference of their phases. If the phase differences are random among the various pieces, the average will be small indicating lack of coherence; but if there is a consistent phase difference among these terms, the average will be larger and its phase will be a measure of that difference. It is therefore natural to make the following definitions:

Two-sided auto-spectrum (real) of series i,

$$S^{(i,i)}_K = s^{(i,i)}_K\ ;$$

Two-sided cross-spectrum (real) of series i and j,

$$S^{(i,j)}_K = |s^{(i,j)}_K|\ ;$$

Phase of two-sided cross spectrum,

$$\Theta^{(i,j)}_K = \tan^{-1}\left[\mathrm{Im}\,s^{(i,j)}_K\,/\mathrm{Re}\,s^{(i,j)}_K\right]\ ;\ \text{and}$$

Two-sided coherence between series i and j,

$$C^{(i,j)}_K = S^{(i,j)}_K\left[S^{(i,i)}_K\,S^{(j,j)}_K\right]^{-1/2}.$$

These definitions apply equally well to positive and negative frequencies (positive and negative K) and

may be thought of as the spectral properties of circularly polarized current components rotating, respectively, in the anti-clockwise and clockwise directions.

The above quantities are readily computed from Fourier coefficients of non-overlapping pieces of any two vector series. They satisfy the usual intuitive and mathematical properties required by analogy with the corresponding one-sided or symmetrical quantities for scalar series. Statistically they also resemble their scalar-series counterparts; if the two vector series are Gaussian, then the autospectrum is distrib-

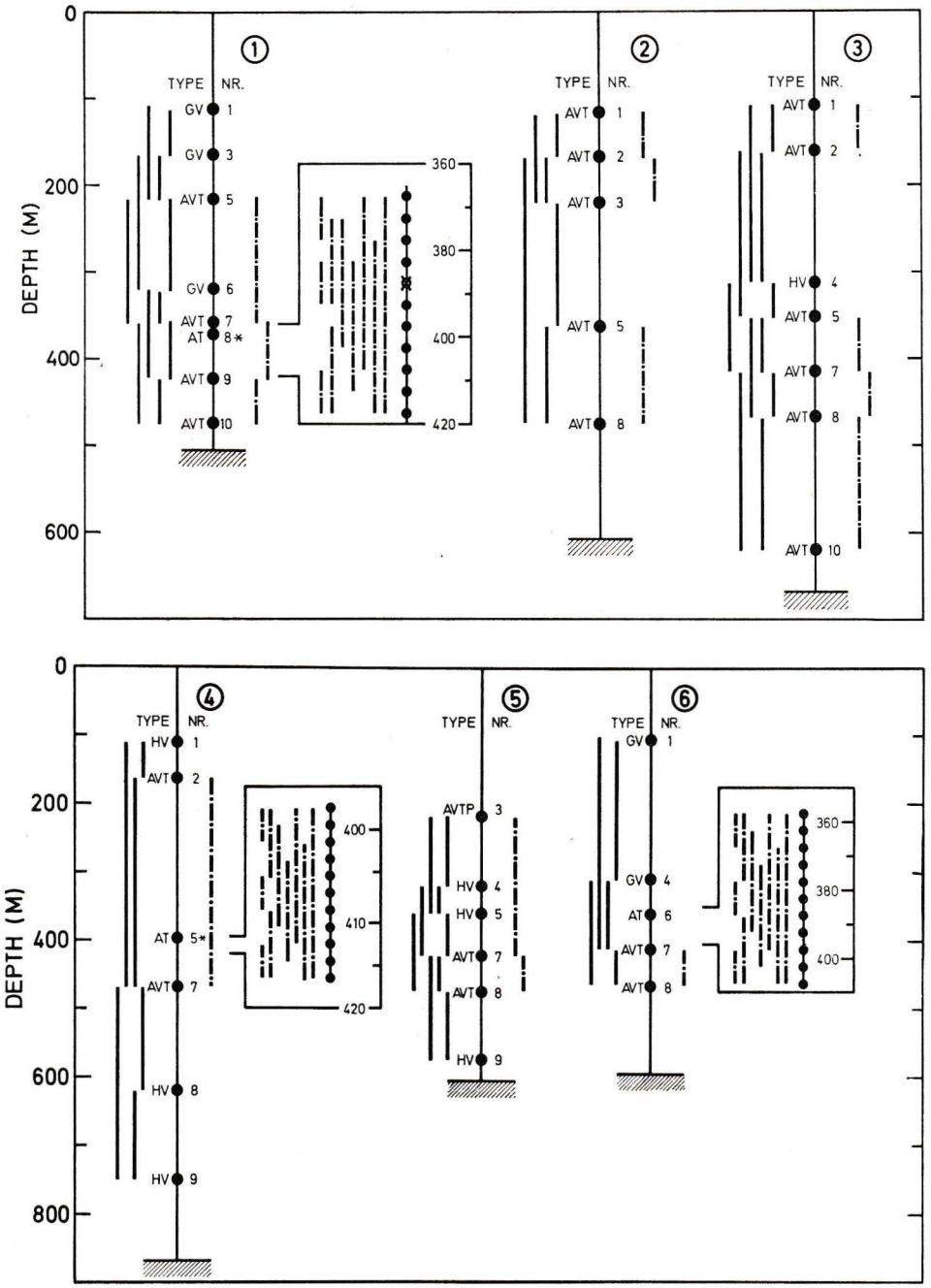

Fig. 7. Locations of instruments on each of the moorings I—VI and the pairs of instruments used to compute coherence for various vertical separations. Solid lines indicate instrument pairs used for current coherences, dashed lines for temperature coherence. Instrument types and the parameters measured by each are given by the legend: A = Aanderaa, G = Geodyne, H = Hydrowerkstätten, V = vector velocity, T = temperature, P = pressure. Thermistor chains are shown by expanded inserts.

Abb. 7. Lage der Instrumente in jeder der Verankerungen I—VI und Instrumentenpaare, die zur Berechnung der Kohärenz für verschiedene Vertikalabstände benutzt wurden. Durchgezogene Linien zeigen Instrumentenpaare für Strömungskohärenzen, gestrichelte Linien für Temperaturkohärenzen. Instrumententypen und gemessene Parameter sind angegeben: A = Aanderaa, G = Geodyne, H = Hydrowerkstätten, V = Geschwindigkeitsvektor, T = Temperatur, P = Druck. Thermistorketten sind vergrößert eingefügt.

uted as chi-squared with 2P degrees of freedom and the coherence distribution is available from tables (AMOS & KOOPMANS 1963).

4 Coherence estimates

From the 34 current meter records alone there are $\binom{34}{2} = 561$ possible pairs from which coherences could be computed with an even larger number available for temperatures. However, a small subset of these possible pairs is sufficient to describe the coherence scales. First are considered quasi-horizontal coherences between instruments on different moorings but at or near the same depth; and second, vertical coherences between instruments on the same mooring. Progressive vector diagrams reveal a strong correlation between the very long term flows at the various moorings. But fluctuations about the mean for instruments on different moorings show no significant coherence for frequencies above 0,02 cph, the minimum resolvable frequency, except at semidiurnal tidal frequency. This is even true between moorings V and III which are nearly colinear in the direction of the mean current and separated by less than 6 km.

Vertically separated instruments show coherence over a wide range of frequencies. Fig. 7 is a summary of the various pairs of instrument locations used in the coherence estimates. Although the instrument pairs are widely distributed throughout the water column and the current itself, instrument separation is the dominant effect on coherences with location of the instruments pair showing no systematic effect. Fig. 8a is typical of the computed coherence between current measurements and fig. 8b of that for temperatures. Note that the coherence decays nearly monotonically away from zero frequency. Also, the frequency ω^*, where the coherence drops below 0.49, the 95% confidence level, is clearly defined. It is therefore possible to define ω^* on the basis of instrument separation alone, independent of the absolute depth of the instrument pair or the particular mooring location.

Figures 9a, b and c are scatter diagrams of ω^* versus instrument separation for the instrument pairs indicated in fig. 7, corresponding respectively to clockwise and counter-clockwise components of coherence for currents and to the conventional coherence for the temperature. The straight line in the figures is that proposed by WEBSTER (1972) as a summary of the current coherence at "Site D". Our current coherence points fall below those of WEBSTER (1972). Note, also, that the clockwise and anticlockwise current coherence plots are nearly indistinguishable; there is no enhanced coherence for currents rotating cum sole. The temperature coherence points in fig. 9c are even further below

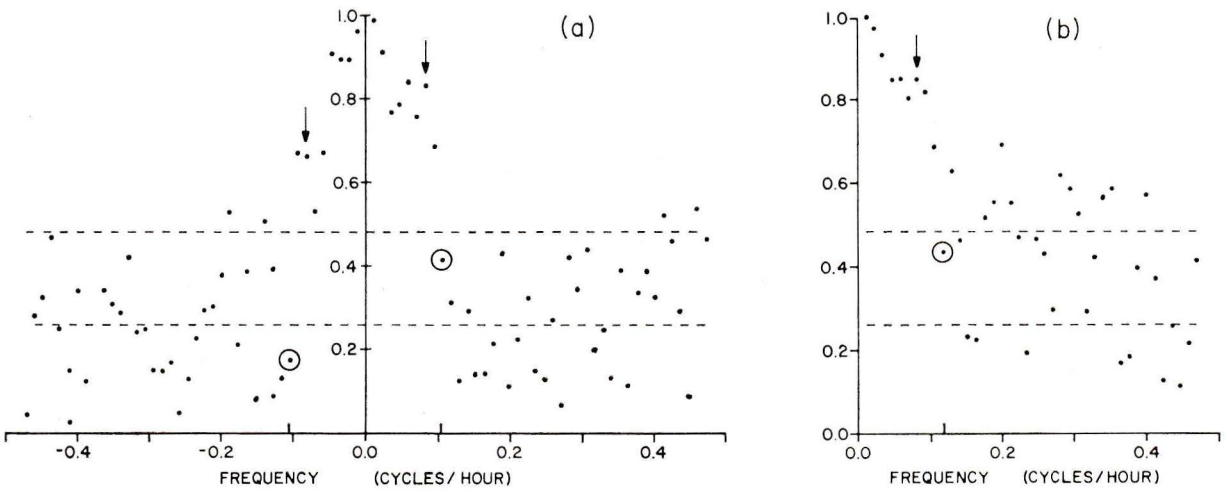

Fig. 8. (a) Coherence vs. frequency between current records at 416 and 467 m on mooring III. The upper dashed line represents the 95% confidence limit and the lower line the expected coherence estimate for incoherent processes. The phase is essentially zero for frequencies where the coherence is significant. Semidiurnal frequency corresponding to semidiurnal period is indicated by arrows. The first point lying below the 95% significance level is encircled and its frequency, called ω^* in the text, is indicated by a tic mark above the frequency axis.
(b) As for (a), but for temperature measurements between thermistors 1 and 5, at 357 and 377 meters respectively on mooring VI.

Abb. 8. (a) Kohärenz als Funktion der Frequenz zwischen den Strömungsmeßreihen in 416 und 467 m Tiefe bei Verankerung III. Die obere gestrichelte Linie gibt die 95%-Konfidenzgrenze wieder, die untere Linie den erwarteten Kohärenz-Schätzwert für inkohärente Prozesse. Die Phase ist im wesentlichen null für Frequenzen, bei denen signifikante Kohärenz auftritt. Die Frequenz zur halbtägigen Periode ist durch Pfeile angezeigt. Der erste Punkt unter der 95%-Konfidenzgrenze ist durch einen Kreis gekennzeichnet, und die zugehörige Frequenz, im Text ω^* genannt, ist auf der Frequenzachse markiert.
(b) Wie bei (a), jedoch für Temperaturmessungen zwischen den Thermistoren 1 und 5 entsprechend den Tiefen 357 bzw. 377 m bei Verankerung VI.

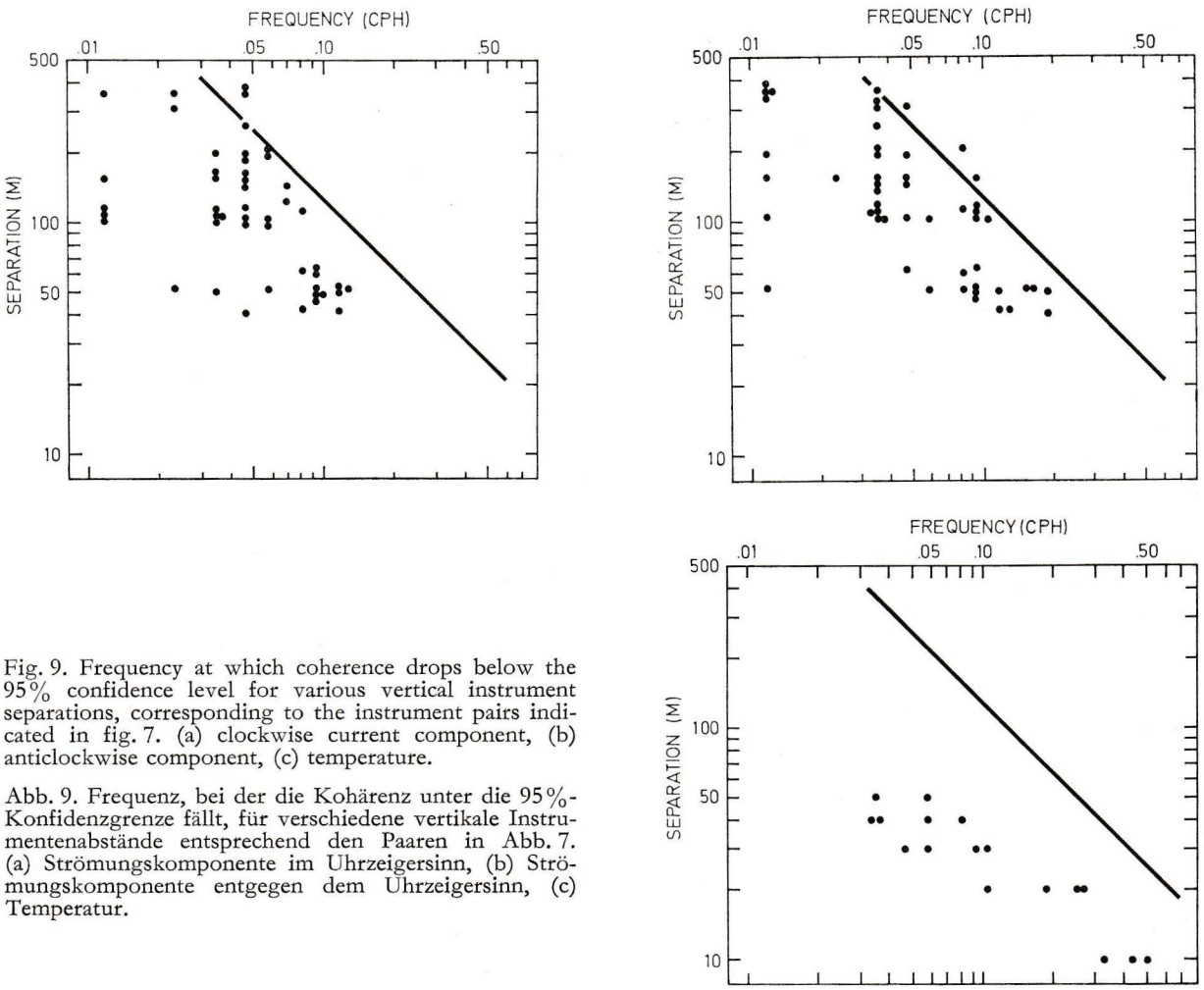

Fig. 9. Frequency at which coherence drops below the 95% confidence level for various vertical instrument separations, corresponding to the instrument pairs indicated in fig. 7. (a) clockwise current component, (b) anticlockwise component, (c) temperature.

Abb. 9. Frequenz, bei der die Kohärenz unter die 95%-Konfidenzgrenze fällt, für verschiedene vertikale Instrumentenabstände entsprechend den Paaren in Abb. 7. (a) Strömungskomponente im Uhrzeigersinn, (b) Strömungskomponente entgegen dem Uhrzeigersinn, (c) Temperatur.

Webster's line, especially those close to the semidiurnal period. This may be at least partially caused by the effect of mooring motion as discussed by Horn & Schott (1975). While current velocities are in error by not more than 0,2 cm/sec due to instrument displacements resulting from (mainly semidiurnal) mooring motion (or 5—10% of current amplitudes at semidiurnal periods), vertical instrument displacements may introduce errors of 20—30% in the temperature fluctuation measurements at semidiurnal periods. The temperature coherence estimates will then be lower due to this contamination by mooring motion whereas vertical current coherence data are hardly affected by this motion.

It can thus be stated that the vertical current coherence in such a region with strong shear flow and sloping bottom is below that observed in typical open ocean conditions, but indicates the same trend of decreasing ω^* for increasing instrument separation. The main purpose of this paper is to present estimates of current and temperature coherence which may be used as a data base for developing an internal wave model for such conditions. It is possible to support the hypothesis of linear wave dynamics in the following way:

The linear equations of motion for internal waves propagating normal to a shear flow, as given for example by Mooers (1975a), imply the ratio r of spectral energy rotating anticlockwise to that rotating clockwise is given by

$$r = \left(\frac{\omega - f'}{\omega + f'}\right)^2$$

where ω is the wave frequency and

$$f' = f + \bar{v}_x + \alpha \bar{v}_z .$$

Here $\bar{v}_x$ and $\bar{v}_z$ are respectively the cross-stream and vertical shears of the geostrophic flow and α is the aspect ratio of the wave, the ratio of horizontal to vertical wave number. With f' and $\bar{v}_z$ both of order 10^{-4} sec^{-1}, the last term will be negligible, and hence r will be largely independent of wavenumber, if $\alpha \ll 1$. Thus, $r \to 0$ for $\omega \to f'$ and $r \approx 1$ for $\omega \gg f'$,

the motion being purely clockwise at frequency f'. As seen in fig. 3, the clockwise component dominates over most of the appropriate frequency range as required. Near f, this relationship does not exist, but the spectral estimates at this frequency are so dominated by leakage from the semidiurnal peak that no positive statement can be made.

5 A note on tidal motion

Semidiurnal tides are evident at all locations and do not follow the description outlined above. Significant coherence at semidiurnal frequency is found between nearly all pairs of instruments having either vertical or horizontal separation, especially in the anticlockwise component. For those record pairs having coherence significant at the 95% level, the phase is typically less than 30 degrees with no apparent systematic behavior. This is consistent with a predominant barotropic tide which has a wavelength large compared to the horizontal scale of the array and is superimposed on the broad spectrum of motions with other frequencies.

In a region with strong shear it may even occur that free internal tidal waves do not exist at all. It has been shown by MAGAARD (1968) and MOOERS (1975a, b), that the frequency range in which free internal waves can exist, normally between the local values of the Brunt-Väisälä frequency N and the inertial frequency f, is modified by the mean flow. The essential change for the low-frequency waves is that their lower limit, f, is replaced, to a good approximation, by $f^* = [f(f + \bar{v}_x)]^{1/2}$. If $\bar{v}_x$ exceeds $0{,}18\,f$, corresponding to a shear of 2×10^{-5} sec^{-1} in table 2, this lower limit is higher than the M_2 tidal frequency. This condition is only intermittently fulfilled in the observation area, as is clear from table 2. It holds over the 42-day average only for pairs during selected time intervals (HORN & SCHOTT 1975). During these intervals, internal semidiurnal tides cannot exist as free internal waves according to the above theories.

Received July 4, 1975

Acknowledgements

The help in sea operations and data processing of the Marine Physics group at the Institute für Meereskunde of Kiel University is gratefully acknowledged. We have benefitted from many discussions with W. HORN. This work was supported by the Deutsche Forschungsgemeinschaft, Bonn-Bad Godesberg.

References

AMOS, D. E. & L. H. KOOPMANS (1963): Tables for the Distribution of the Coefficient of Coherence for Stationary Bivariate Gaussian Processes. — Sandia Corporation, 327 pp. Available from: Clearinghouse, National Bureau of Standards, Springfield, Va. 22151.

DIETRICH, G. & W. HORN (1973): Norwegian Sea-Expedition 1969. — „Meteor" Forsch.-Ergebn. A, 12: 1—10.

FOFONOFF, N. P. (1969): Spectral Characteristics of Internal Waves in the Ocean. — Deep-Sea Res., **16** supp.: 59—71.

GARRETT, C. & W. MUNK (1972): Space-Time Scales of Internal Waves. — Geophysical Fluid Dyn. **3**: 225—264.

— — (1975): Space-Time Scales of Internal Waves: A Progress Report. — J. Geophys. Res. **80** (3): 291—297.

GONELLA, J. (1972): A Rotary-Component Method for Analysing Meteorological and Oceanographic Vector Time Series. — Deep-Sea Res. **19**: 833—846.

HORN, W. & F. SCHOTT (1976): Measurements of stratification and currents at the Norwegian Continental Slope. — „Meteor" Forsch.-Ergebn. A, 17: 23—63.

MAGAARD, L. (1968): Ein Beitrag zur Theorie der internen Wellen als Störungen geostrophischer Strömungen. — Dt. Hydrographische Z. **21** (6): 241—278.

MOOERS, C. N. K. (1973): A Technique for the Cross Spectrum Analysis of Pairs of Complex-Valued Time Series, with Emphasis on Properties of Polarized Components and Rotational Invariants. — Deep-Sea Res. **20**: 1129—1141.

— (1975a): Several Effects of a Baroclinic Current on the Cross-Stream Propagation of Internal-Inertial Wave. — Geophysical Fluid Dyn. **6**: 245—276.

— (1975b): Several Effects of Baroclinic Currents on the Three-Dimensional Propagation of Inertial-Internal Waves. — Geophysical Fluid Dyn. **6**: 277—285.

SIEDLER, G. (1974): Observations of Internal Wave Coherence in the Deep Ocean. — Deep-Sea Res. **21**: 597—610.

WEBSTER, F. (1972): Estimates of the Coherence of Ocean Currents over Vertical Distances. — Deep-Sea Res. **19**: 35—44.